



## Seasonal variability in methane and nitrous oxide fluxes from tropical peatlands in the western Amazon basin

Yit Arn Teh<sup>1</sup>, Wayne A. Murphy<sup>2</sup>, Juan-Carlos Berrio<sup>2</sup>, Arnoud Boom<sup>2</sup>, and Susan E. Page<sup>2</sup>

<sup>1</sup>Institute of Biological and Environmental Sciences, University of Aberdeen, Aberdeen, UK

<sup>2</sup>Department of Geography, University of Leicester, Leicester, UK

Correspondence to: Yit Arn Teh (yateh@abdn.ac.uk)

Received: 14 February 2017 – Discussion started: 24 February 2017

Revised: 25 May 2017 – Accepted: 14 June 2017 – Published: 7 August 2017

**Abstract.** The Amazon plays a critical role in global atmospheric budgets of methane (CH<sub>4</sub>) and nitrous oxide (N<sub>2</sub>O). However, while we have a relatively good understanding of the continental-scale flux of these greenhouse gases (GHGs), one of the key gaps in knowledge is the specific contribution of peatland ecosystems to the regional budgets of these GHGs. Here we report CH<sub>4</sub> and N<sub>2</sub>O fluxes from lowland tropical peatlands in the Pastaza–Marañón foreland basin (PMFB) in Peru, one of the largest peatland complexes in the Amazon basin. The goal of this research was to quantify the range and magnitude of CH<sub>4</sub> and N<sub>2</sub>O fluxes from this region, assess seasonal trends in trace gas exchange, and determine the role of different environmental variables in driving GHG flux. Trace gas fluxes were determined from the most numerically dominant peatland vegetation types in the region: forested vegetation, forested (short pole) vegetation, *Mauritia flexuosa*-dominated palm swamp, and mixed palm swamp. Data were collected in both wet and dry seasons over the course of four field campaigns from 2012 to 2014. Diffusive CH<sub>4</sub> emissions averaged  $36.05 \pm 3.09$  mg CH<sub>4</sub>-C m<sup>-2</sup> day<sup>-1</sup> across the entire dataset, with diffusive CH<sub>4</sub> flux varying significantly among vegetation types and between seasons. Net ebullition of CH<sub>4</sub> averaged  $973.3 \pm 161.4$  mg CH<sub>4</sub>-C m<sup>-2</sup> day<sup>-1</sup> and did not vary significantly among vegetation types or between seasons. Diffusive CH<sub>4</sub> flux was greatest for mixed palm swamp ( $52.0 \pm 16.0$  mg CH<sub>4</sub>-C m<sup>-2</sup> day<sup>-1</sup>), followed by *M. flexuosa* palm swamp ( $36.7 \pm 3.9$  mg CH<sub>4</sub>-C m<sup>-2</sup> day<sup>-1</sup>), forested (short pole) vegetation ( $31.6 \pm 6.6$  mg CH<sub>4</sub>-C m<sup>-2</sup> day<sup>-1</sup>), and forested vegetation ( $29.8 \pm 10.0$  mg CH<sub>4</sub>-C m<sup>-2</sup> day<sup>-1</sup>). Diffusive CH<sub>4</sub> flux also showed marked seasonality, with diver-

gent seasonal patterns among ecosystems. Forested vegetation and mixed palm swamp showed significantly higher dry season ( $47.2 \pm 5.4$  mg CH<sub>4</sub>-C m<sup>-2</sup> day<sup>-1</sup> and  $85.5 \pm 26.4$  mg CH<sub>4</sub>-C m<sup>-2</sup> day<sup>-1</sup>, respectively) compared to wet season emissions ( $6.8 \pm 1.0$  mg CH<sub>4</sub>-C m<sup>-2</sup> day<sup>-1</sup> and  $5.2 \pm 2.7$  mg CH<sub>4</sub>-C m<sup>-2</sup> day<sup>-1</sup>, respectively). In contrast, forested (short pole) vegetation and *M. flexuosa* palm swamp showed the opposite trend, with dry season flux of  $9.6 \pm 2.6$  and  $25.5 \pm 2.9$  mg CH<sub>4</sub>-C m<sup>-2</sup> day<sup>-1</sup>, respectively, versus wet season flux of  $103.4 \pm 13.6$  and  $53.4 \pm 9.8$  mg CH<sub>4</sub>-C m<sup>-2</sup> day<sup>-1</sup>, respectively. These divergent seasonal trends may be linked to very high water tables (> 1 m) in forested vegetation and mixed palm swamp during the wet season, which may have constrained CH<sub>4</sub> transport across the soil–atmosphere interface. Diffusive N<sub>2</sub>O flux was very low ( $0.70 \pm 0.34$  μg N<sub>2</sub>O–N m<sup>-2</sup> day<sup>-1</sup>) and did not vary significantly among ecosystems or between seasons. We conclude that peatlands in the PMFB are large and regionally significant sources of atmospheric CH<sub>4</sub> that need to be better accounted for in regional emissions inventories. In contrast, N<sub>2</sub>O flux was negligible, suggesting that this region does not make a significant contribution to regional atmospheric budgets of N<sub>2</sub>O. The divergent seasonal pattern in CH<sub>4</sub> flux among vegetation types challenges our underlying assumptions of the controls on CH<sub>4</sub> flux in tropical peatlands and emphasizes the need for more process-based measurements during periods of high water table.

## 1 Introduction

The Amazon basin plays a critical role in the global atmospheric budgets of carbon (C) and greenhouse gases (GHGs) such as methane (CH<sub>4</sub>) and nitrous oxide (N<sub>2</sub>O). Recent basin-wide studies suggest that the Amazon as a whole accounts for approximately 7% of global atmospheric CH<sub>4</sub> emissions (Wilson et al., 2016). N<sub>2</sub>O emissions are of a similar magnitude, with emissions ranging from 2 to 3 Tg N<sub>2</sub>O–N yr<sup>-1</sup> (or approximately 12–18% of global atmospheric emissions) (Huang et al., 2008; Saikawa et al., 2013, 2014). While we have a relatively strong understanding of the role that the Amazon plays in regional and global atmospheric budgets of these gases, one of the key gaps in knowledge is the contribution of specific ecosystem types to regional fluxes of GHGs (Huang et al., 2008; Saikawa et al., 2013, 2014). In particular, our understanding of the contribution of Amazonian wetlands to regional C and GHG budgets is weak, as the majority of past ecosystem-scale studies have focused on *terra firme* forests and savannas (D'Amelio et al., 2009; Saikawa et al., 2013; Wilson et al., 2016; Kirschke et al., 2013; Nisbet et al., 2014). Empirical studies of GHG fluxes from Amazonian wetlands are more limited in geographic scope and have focused on three major areas: wetlands in the state of Amazonas near the city of Manaus (Devol et al., 1990; Bartlett et al., 1988, 1990; Keller et al., 1986), the Pantanal region (Melack et al., 2004; Marani and Alvalá, 2007; Lienggaard et al., 2013), and the Orinoco River basin (Smith et al., 2000; Lavelle et al., 2014). Critically, none of the ecosystems sampled in the past were peat-forming ones; rather, the habitats investigated were non-peat-forming (i.e., mineral or organo-mineral soils), seasonally inundated floodplain forests (i.e., *varzea*), rivers, or lakes.

Peatlands are one of the major wetland habitats absent from current bottom-up GHG inventories for the Amazon basin and are often grouped together with non-peat-forming wetlands in regional atmospheric budgets (Wilson et al., 2016). Unlike their Southeast Asian counterparts, most peatlands in the Amazon basin are unaffected by human activity at the current time (Lahteenoja et al., 2009a, b; Lahteenoja and Page, 2011), except for ecosystems in the Madre de Dios region in southeastern Peru, which are impacted by gold mining (Householder et al., 2012). Because we have little or no data on ecosystem-level land–atmosphere fluxes from Amazonian peatlands (Lahteenoja et al., 2009b, 2012; Kirschke et al., 2013; Nisbet et al., 2014), it is difficult to ascertain if rates of GHG flux from these ecosystems are similar to or different from mineral soil wetlands (e.g., *varzea*). Given that underlying differences in plant community composition and soil properties are known to modulate the cycling and flux of GHGs in wetlands (Limpens et al., 2008; Melton et al., 2013; Belyea and Baird, 2006; Sjögersten et al., 2014), expanding our observations to include a wider range of wetland habitats is critical in order to improve our understanding of regional trace gas exchange and also to determine whether ag-

gregating peat and mineral soil wetlands together in bottom-up emissions inventories are appropriate for regional budget calculations. Moreover, Amazonian peatlands are thought to account for a substantial land area (i.e., up to 150 000 km<sup>2</sup>) (Schulman et al., 1999; Lahteenoja et al., 2012), and any differences in biogeochemistry among peat and mineral/organomineral soil wetlands may therefore have important implications for understanding and modeling the biogeochemical functioning of the Amazon basin as a whole.

Since the identification of extensive peat forming wetlands in the north (Lahteenoja et al., 2009a, b; Lahteenoja and Page 2011) and south (Householder et al., 2012) of the Peruvian Amazon, several studies have been undertaken to better characterize these habitats, investigating vegetation composition and habitat diversity (Draper et al., 2014; Kelly et al., 2014; Householder et al., 2012; Lahteenoja and Page, 2011), vegetation history (Lahteenoja and Roucoux, 2010), C stocks (Lahteenoja et al., 2012; Draper et al., 2014), hydrology (Kelly et al., 2014), and peat chemistry (Lahteenoja et al., 2009a, b). Most of the studies have focused on the Pastaza–Marañón foreland basin (PMFB), where one of the largest stretches of contiguous peatlands has been found (Lahteenoja et al. 2009a; Lahteenoja and Page, 2011; Kelly et al., 2014), covering an estimated area of 35 600 ± 2133 km<sup>2</sup> (Draper et al., 2014). Up to 90% of the peatlands in the PMFB lie in flooded backwater river margins on floodplains and are influenced by large, annual fluctuations in water table caused by the Amazonian flood pulse (Householder et al., 2012; Lahteenoja et al., 2009a). These floodplain systems are dominated by peat deposits that range in depth from ~3.9 m (Lahteenoja et al., 2009a) to ~12.9 m (Householder et al., 2012). The remaining 10% of these peatlands are not directly influenced by river flow and form domed (i.e., raised) nutrient-poor bogs that likely only receive water and nutrients from rainfall (Lahteenoja et al., 2009b). These nutrient-poor bogs are dominated by large, C-rich forests (termed “pole forests”) that represent a very-high-density C store (total pool size of 1391 ± 710 Mg C ha<sup>-1</sup>, which includes both above- and belowground stocks), exceeding even the C density of nearby floodplain systems (Draper et al., 2014). Even though the peats in these nutrient-poor bogs have a relatively high hydraulic conductivity, they act as natural stores of water because of high rainwater inputs (> 3000 mm per annum), which help to maintain high water tables, even during parts of the dry season (Kelly et al., 2014).

CH<sub>4</sub> flux in tropical soils are regulated by the complex interplay among multiple factors that regulate CH<sub>4</sub> production, oxidation, and transport. Key factors include redox/water table depth (Couwenberg et al., 2010, 2011; Silver et al., 1999; Teh et al., 2005; von Fischer and Hedin, 2007), plant productivity (von Fischer and Hedin, 2007; Whiting and Chanton, 1993), soil organic matter lability (Wright et al., 2011), competition for C substrates among anaerobes (Teh et al., 2008; Teh and Silver, 2006; von Fischer and Hedin, 2007), and presence of plants capable of facilitating atmospheric egress

(Pangala et al., 2013). Of all these factors, fluctuation in soil redox conditions, as mediated by variations in water table depth, is perhaps most critical in regulating CH<sub>4</sub> dynamics (Couwenberg et al., 2010, 2011) because of the underlying physiology of the microbes that produce and consume CH<sub>4</sub>. Methanogenic archaea are obligate anaerobes that only produce CH<sub>4</sub> under anoxic conditions (Conrad, 1996); as a consequence, they are only active in stably anoxic soil microsites or soil layers, where they are protected from the effects of strong oxidants such as oxygen or where competition for reducing equivalents (e.g., acetate, H<sub>2</sub>) from other anaerobic microorganisms is eliminated (Teh et al., 2005, 2008; Teh and Silver, 2006; von Fischer and Hedin, 2002, 2007). CH<sub>4</sub> oxidation, in contrast, is thought to be driven primarily by aerobic methanotrophic bacteria in tropical soils (Hanson and Hanson, 1996; Teh et al., 2005, 2006; von Fischer and Hedin, 2002, 2007), with anaerobic CH<sub>4</sub> oxidation playing a quantitatively smaller role (Blazewicz et al., 2012). Thus, fluctuations in redox or water table depth play a fundamental role in directing the flow of C among different anaerobic pathways (Teh et al., 2008; Teh and Silver, 2006; von Fischer and Hedin, 2007), and shifting the balance between production and consumption of CH<sub>4</sub> (Teh et al., 2005; von Fischer and Hedin, 2002). Moreover, water table or soil moisture fluctuations are also thought to profoundly influence CH<sub>4</sub> transport dynamics throughout the soil profile, changing the relative partitioning of CH<sub>4</sub> among different transport pathways such as diffusion, ebullition, and plant-facilitated transport (Whalen, 2005; Jungkunst and Fiedler, 2007).

Controls on N<sub>2</sub>O flux are also highly complex (Groffman et al., 2009), with N<sub>2</sub>O originating from as many as four separate sources (e.g., bacterial ammonia oxidation, archaeal ammonia oxidation, denitrification, dissimilatory nitrate reduction to ammonium), each with different environmental controls (Baggs, 2008; Morley and Baggs, 2010; Firestone and Davidson, 1989; Firestone et al., 1980; Pett-Ridge et al., 2013; Silver et al., 2001; Prosser and Nicol, 2008). Key factors regulating soil N<sub>2</sub>O flux include redox, soil moisture content or water table depth, temperature, pH, labile C availability, and labile N availability (Groffman et al., 2009). As is the case for CH<sub>4</sub>, variations in redox/water table depth play an especially prominent role in regulating N<sub>2</sub>O flux in tropical peatland ecosystems because all of the processes that produce N<sub>2</sub>O are redox-sensitive, with bacterial or archaeal ammonia oxidation occurring under aerobic conditions (Prosser and Nicol, 2008; Firestone and Davidson, 1989; Firestone et al., 1980) whereas nitrate-reducing processes (i.e., denitrification, dissimilatory nitrate reduction to ammonium) occur under anaerobic ones (Firestone and Davidson, 1989; Firestone et al., 1980; Morley and Baggs, 2010; Silver et al., 2001). Moreover, for nitrate-reducing processes, which are believed to be the dominant source of N<sub>2</sub>O in wet systems, the extent of anaerobiosis also controls the relative proportion of N<sub>2</sub>O or N<sub>2</sub> produced during dissimilatory metabolism

(Firestone and Davidson, 1989; Firestone et al., 1980; Morley and Baggs, 2010; Silver et al., 2001).

In order to improve our understanding of the biogeochemistry and rates of GHG exchange from Amazonian peatlands, we conducted a preliminary study of CH<sub>4</sub> and N<sub>2</sub>O fluxes from forested peatlands in the PMFB. The main objectives of this are to

1. quantify the magnitude and range of soil CH<sub>4</sub> and N<sub>2</sub>O fluxes from a subset of peatlands in the PMFB that represent dominant vegetation types;
2. determine seasonal patterns of trace gas exchange;
3. establish the relationship between trace gas fluxes and environmental variables.

Sampling was concentrated on the four most dominant vegetation types in the area, based on prior work by the investigators (Lahteenoja and Page, 2011). Trace gas fluxes were captured from both floodplain systems and nutrient-poor bogs in order to account for underlying differences in biogeochemistry that may arise from variations in hydrology. Sampling was conducted during four field campaigns (two wet season, two dry season) over a 27-month period, extending from February 2012 to May 2014.

## 2 Materials and methods

### 2.1 Study site and sampling design

The study was carried out in the lowland tropical peatland forests of the PMFB, between 2 and 35 km south of the city of Iquitos, Peru (Lahteenoja et al., 2009a, b) (Fig. 1, Table 1). The mean annual temperature is 26 °C, annual precipitation is ca. 3100 mm, relative humidity ranges from 80 to 90 %, and altitude ranges from ca. 90 to 130 m a.s.l. (above sea level) (Marengo 1998). The northwestern Amazon basin near Iquitos experiences pronounced seasonality, which is characterized by consistently high annual temperatures, but marked seasonal variation in precipitation (Tian et al., 1998) and an annual river flood pulse linked to seasonal discharge from the Andes (Junk, 1989). Precipitation events are frequent, intense and of significant duration during the wet season (November to May) and infrequent, intense, and of short duration during the dry season (June to August). September and October represent a transitional period between dry and wet seasons, where rainfall patterns are less predictable. Catchments in this region receive no less than 100 mm of rain per month (Espinoza Villar et al., 2009a, b) and > 3000 mm of rain per year. River discharge varies by season, with the lowest discharge between the dry season months of August and September. Peak discharge from the wet season flood pulse occurs between April and May, as recorded at the Tamshiyacu River gauging station (Espinoza Villar et al., 2009b).

**Table 1.** Site characteristics including field site location, nutrient status, plot, and flux chamber replication.

Vegetation type	Site name	Nutrient status*	Latitude (S)	Longitude (W)	Plots	Flux chambers
Forested	Buena Vista	Rich	4°14'45.60" S	73°12'0.20" W	21	105
Forested (short pole)	San Jorge (center)	Poor	4°03'35.95" S	73°12'01.13" W	6	28
Forested (short pole)	Miraflores	Poor	4°28'16.59" S	74°4'39.95" W	41	204
<i>M. flexuosa</i> Palm Swamp	Quistococha	Intermediate	3°49'57.61" S	73°12'01.13" W	135	668
<i>M. flexuosa</i> Palm Swamp	San Jorge (edge)	Intermediate	4°03'18.83" S	73°10'16.80" W	18	86
Mixed palm swamp	Charo	Rich	4°16'21.80" S	73°15'27.80" W	18	90

\* After Householder et al. (2012) and Lahteenoja et al. (2009a, b).

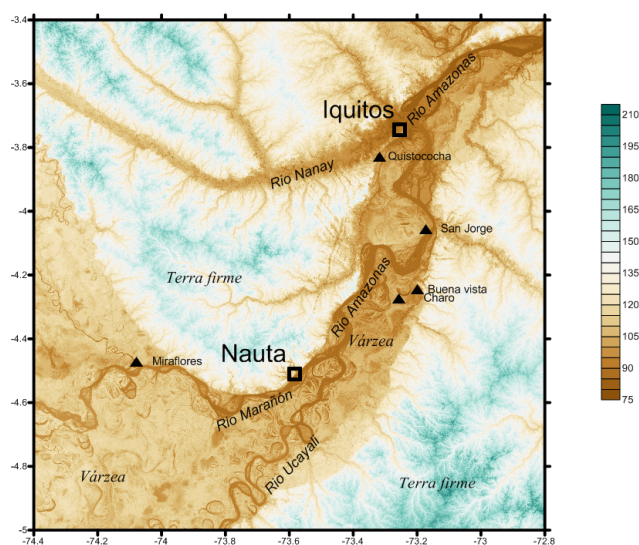


**Figure 1.** Map of the study region and field sites. The color scale to the right of the map denotes elevation in m.a.s.l. Tan and brown tones indicate areas in which peatlands are found; however, not all of these areas are peatland-dominated.

Histosols form the dominant soil type for peatlands in this region (Andriess, 1988; Lahteenoja and Page, 2011). Study sites are broadly classified as nutrient-rich, intermediate, or nutrient-poor (Lahteenoja and Page, 2011), with pH ranging from 3.5 to 7.2 (Lahteenoja and Page, 2011; Lahteenoja et al., 2009a, b). More specific data on pH for our plots are presented in Table 3. Nutrient-rich (i.e., minerotrophic) sites tend to occur on floodplains and river margins and account for at least 60% of the peatland cover in the PMFB (Lahteenoja and Page, 2011; Draper et al., 2014). They receive water, sediment, and nutrient inputs from the annual Amazon river flood pulse (Householder et al., 2012; Lahteenoja and Page, 2011), leading to higher inorganic nutrient content, of which Ca and other base cations form major constituents (Lahteenoja and Page, 2011). Many of the soils in these nutrient-rich areas are fluvaquentic Tropofibrists (Andriess, 1988) and contain thick mineral layers or minerogenic intrusions, reflective of episodic sedimentation events

in the past (Lahteenoja and Page, 2011). In contrast, nutrient-poor (i.e., oligotrophic) sites tend to occur further inland (Lahteenoja and Page, 2011; Draper et al., 2014). They are almost entirely rain-fed and receive low or infrequent inputs of water and nutrients from streams and rivers (Lahteenoja and Page, 2011). These ecosystems account for 10 to 40% of peatland cover in the PMFB, though precise estimates vary depending on the land classification scheme employed (Lahteenoja and Page, 2011; Draper et al., 2014). Soil Ca and base cation concentrations are significantly lower in these sites compared to nutrient-rich ones, with similar concentrations to that of rainwater (Lahteenoja and Page, 2011). Soils are classified as typic or hydric Tropofibrists (Andriess, 1988). Even though Ca and base cations themselves play no direct role in modulating CH<sub>4</sub> and N<sub>2</sub>O fluxes, underlying differences in soil fertility may indirectly influence CH<sub>4</sub> and N<sub>2</sub>O flux by influencing the rate of labile C input to the soil, the decomposability of organic matter, and the overall throughput of C and nutrients through the plant–soil system (Firestone and Davidson, 1989; Groffman et al., 2009; von Fischer and Hedin, 2007; Whiting and Chanton, 1993).

We established 239 sampling plots (~30 m<sup>2</sup> per plot) within five tropical peatland sites that captured four of the dominant vegetation types in the region (Draper et al., 2014; Householder et al., 2012; Kelly et al., 2014; Lahteenoja and Page, 2011) and which encompassed a range of nutrient availabilities (Fig. 1, Table 1) (Lahteenoja and Page, 2011; Lahteenoja et al., 2009a). These four dominant vegetation types included forested vegetation (nutrient-rich;  $n = 21$  plots), forested (short pole) vegetation (nutrient-poor;  $n = 47$  plots), *Mauritia flexuosa*-dominated palm swamp (intermediate fertility;  $n = 153$  plots), and mixed palm swamp (nutrient-rich;  $n = 18$  plots) (Table 1). Four of the study sites (Buena Vista, Charo, Miraflores, and Quistococha) were dominated by only one vegetation type, whereas San Jorge contained a mixture of *M. flexuosa* palm swamp and forested (short pole) vegetation (Table 1). As a consequence, both vegetation types were sampled in San Jorge to develop a more representative picture of GHG fluxes from this location. Sampling efforts were partially constrained by issues of site access; some locations were difficult to access (e.g., cen-

tre of the San Jorge peatland) due to water table height and navigability of river channels; as a consequence, sampling patterns were somewhat uneven, with higher sampling densities in some peatlands than in others (Table 1).

In each peatland site, transects were established from the edge of the peatland to its center. Each transect varied in length from 2 to 5 km, depending on the relative size of the peatland. Randomly located sampling plots ( $\sim 30 \text{ m}^2$  per plot) were established at 50 or 200 m intervals along each transect, from which GHG fluxes and environmental variables were measured concomitantly. The sampling interval (i.e., 50 or 200 m) was determined by the length of the transect or size of the peatland, with shorter sampling intervals (50 m) for shorter transects (i.e., smaller peatlands) and longer sampling intervals (200 m) for longer transects (i.e., larger peatlands).

## 2.2 Quantifying soil–atmosphere exchange

Soil–atmosphere fluxes ( $\text{CH}_4$ ,  $\text{N}_2\text{O}$ ) were determined in four campaigns over a 2-year annual water cycle: February 2012 (wet season), June–August 2012 (dry season), June–July 2013 (dry season), and May–June 2014 (wet season). The duration of the campaign for each study site varied depending on its size. Each study site was generally sampled only once for each campaign, except for a subset of plots within each vegetation type where diurnal studies were conducted to determine whether  $\text{CH}_4$  and  $\text{N}_2\text{O}$  fluxes varied over daily time steps. Gas exchange was quantified using a floating static chamber approach (Livingston and Hutchinson, 1995; Teh et al., 2011). Static flux measurements were made by enclosing a  $0.225 \text{ m}^2$  area with a dark, single component, vented 10 L flux chamber. No chamber bases (collars) were used due to the highly saturated nature of the soils. In most cases, a standing water table was present at the soil surface, so chambers were placed directly onto the water. In the absence of a standing water table, a weighted skirt was applied to create an airtight seal. Under these drier conditions, chambers were placed carefully on the soil surface. In order to reduce the risk of pressure-induced ebullition or disruption to soil gas concentration profiles caused by the investigators' footfall, flux chambers were lowered from a distance of 2 m away using a 2 m long pole. Gas samples were collected with syringes using  $> 2 \text{ m}$  lengths of Tygon<sup>®</sup> tubing, after thoroughly purging the dead volumes in the sample lines. To promote even mixing within the headspace, chambers were fitted with small computer fans (Pumpanen et al., 2004). Headspace samples were collected from each flux chamber at five intervals over a 25 min enclosure period using a gas-tight syringe. Gas samples were stored in evacuated Exetainers<sup>®</sup> (Labco Ltd., Lampeter, UK), shipped to the UK, and subsequently analyzed for  $\text{CH}_4$ ,  $\text{CO}_2$ , and  $\text{N}_2\text{O}$  concentrations using Thermo TRACE GC Ultra (Thermo Fisher Scientific Inc., Waltham, Massachusetts, USA) at the University of St. Andrews. Chromatographic separation was achieved

using a Poropak-Q column, and gas concentrations were determined using a flame ionization detector (FID) for  $\text{CH}_4$ , a methanizer-FID for  $\text{CO}_2$ , and an electron capture detector (ECD) for  $\text{N}_2\text{O}$ . Instrumental precision, determined from repeated analysis of standards, was  $< 5 \%$  for all detectors.

Diffusive fluxes were determined by using the JMP IN version 11 (SAS Institute, Inc., Cary, North Carolina, USA) statistical package to plot best-fit lines to the data for headspace concentration against time for individual flux chambers, with fluxes calculated from linear or nonlinear regressions depending on the individual concentration trend against time (Teh et al., 2014). Gas mixing ratios (ppm) were converted to areal fluxes by using the ideal gas law to solve for the quantity of gas in the headspace (on a mole or mass basis) and normalized by the surface area of each static flux chamber (Livingston and Hutchinson, 1995). Ebullition-derived  $\text{CH}_4$  fluxes were also quantified in our chambers where evidence of ebullition was found. This evidence consisted of either (i) rapid, nonlinear increases in  $\text{CH}_4$  concentration over time; (ii) abrupt, stochastic increases in  $\text{CH}_4$  concentration over time; or (iii) an abrupt stochastic increase in  $\text{CH}_4$  concentration, followed by a linear decline in concentration. For observations following pattern (i), flux was calculated by fitting a quadratic regression equation to the data ( $P < 0.05$ ), and  $\text{CH}_4$  flux determined from the initial steep rise in  $\text{CH}_4$  concentration. For data following pattern (ii), the ebullition rate was determined by calculating the total  $\text{CH}_4$  production over the course of the bubble event, in line with prior work conducted by the investigators (Teh et al., 2011). Last, for data following pattern (iii), a best-fit line was plotted to the  $\text{CH}_4$  concentration data after the bubble event and a net rate of  $\text{CH}_4$  uptake calculated from the gradient of the line. While observations (i)–(iii) all reflect the effects of ebullition, only observations following patterns (i) and (ii) indicate net emission to the atmosphere, whereas observations following pattern (iii) indicate emission followed by net uptake. As a consequence, patterns (i) and (ii) were categorized as “net ebullition” (i.e., net efflux) whereas observations following pattern (iii) were categorized as “ebullition-driven  $\text{CH}_4$  uptake” (i.e., net influx).

## 2.3 Environmental variables

To investigate the effects of environmental variables on trace gas fluxes, we determined air temperature, soil temperature, chamber headspace temperature, soil pH, soil electrical conductivity (EC;  $\mu\text{S m}^{-2}$ ), dissolved oxygen concentration of the soil pore water (DO; measured as percent saturation, %) in the top 15 cm of the peat column, and water table position concomitant with gas sampling. Air temperature (measured 1.3 m above the soil) and chamber headspace temperature were measured using a Checktemp<sup>®</sup> probe and meter (Hanna Instruments LTD, Leighton Buzzard, UK). Peat temperature, pH, DO, and EC were measured at a depth of 15 cm below the peat surface and recorded in situ with each gas sample

**Table 2.** Proportion of observations for each vegetation type that showed evidence of ebullition, mean rates of ebullition, and ebullition-driven CH<sub>4</sub> uptake. Values represent means and standard errors.

Vegetation type	Percentage of observations (%)	Net ebullition (mg CH <sub>4</sub> -C m <sup>-2</sup> day <sup>-1</sup> )		Ebullition-driven uptake (mg CH <sub>4</sub> -C m <sup>-2</sup> day <sup>-1</sup> )	
		Wet season	Dry season	Wet season	Dry season
Forested	10.5	0	0	0	-136.4 ± 0.1
Forested (short pole)	6.9	994.6 ± 293.2	512.5 ± 153.0	-95.8 ± 0.0	-245.5 ± 48.9
<i>M. flexuosa</i> palm swamp	16.7	1192.0 ± 305.7	994.3 ± 237.3	-869.4 ± 264.8	-401.4 ± 59.9
Mixed palm swamp	12.2	0	733.6 ± 313.1	0	-464.4 ± 565.9

using a HACH® rugged outdoor HQ30D multimeter and pH, DO, or EC probe. At sites where the water level was above the peat surface, the water depth was measured using a meter rule. Where the water table was at or below the peat surface, the water level was measured by auguring a hole to 1 m depth and measuring water table depth using a meter rule.

## 2.4 Statistical analyses

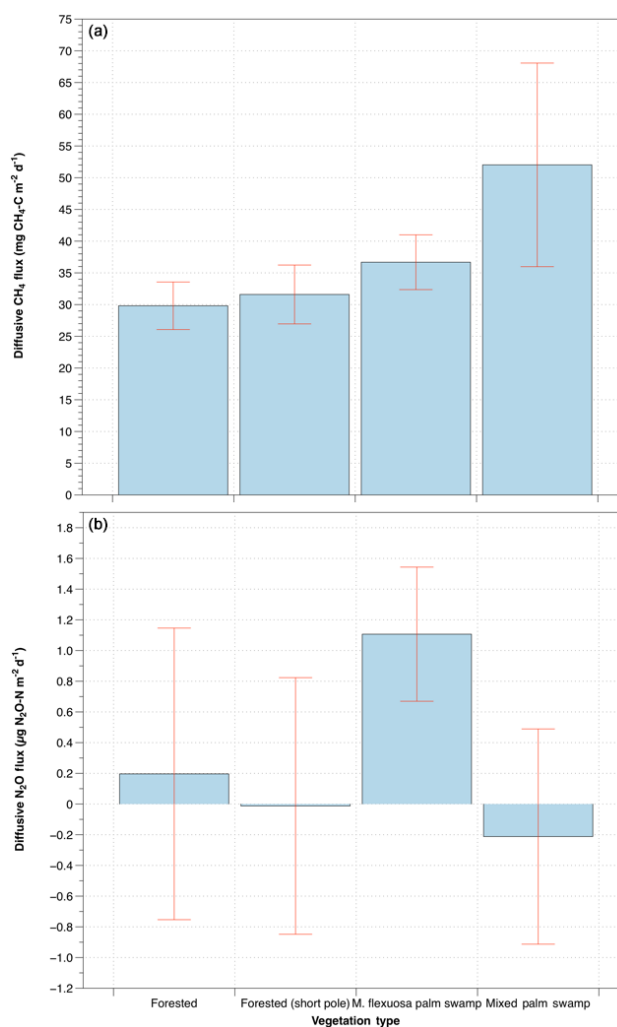
Statistical analyses were performed using JMP IN version 11 (SAS Institute, Inc., Cary, North Carolina, USA). Box-Cox transformations were applied where the data failed to meet the assumptions of analysis of variance (ANOVA); otherwise, nonparametric tests were applied (e.g., Wilcoxon signed-rank test). ANOVA and analysis of co-variance (ANCOVA) were used to test for relationships between gas fluxes and vegetation type, season, and environmental variables. When determining the effect of vegetation type on gas flux, data from different study sites (e.g., San Jorge and Miraflores) were pooled together. Means comparisons were tested using Fisher's least significant difference (LSD) test.

## 3 Results

### 3.1 Differences in gas fluxes and environmental variables among vegetation types

All vegetation types were net sources of CH<sub>4</sub>, with an overall mean (± SE – standard error) diffusive flux of 36.1 ± 3.1 mg CH<sub>4</sub>-C m<sup>-2</sup> day<sup>-1</sup> and a mean net ebullition flux of 973.3 ± 161.4 mg CH<sub>4</sub>-C m<sup>-2</sup> day<sup>-1</sup> (Fig. 2, Table 2). We also saw examples of ebullition-driven CH<sub>4</sub> uptake (i.e., a sudden or stochastic increase in CH<sub>4</sub> concentration, followed immediately by a rapid linear decline in concentration), with a mean rate of -504.1 ± 84.4 mg CH<sub>4</sub>-C m<sup>-2</sup> day<sup>-1</sup> (Table 2). Diffusive fluxes of CH<sub>4</sub> accounted for the majority of observations (83.3 to 93.1 %), while ebullition fluxes accounted for a much smaller proportion of observations (6.9 to 16.7 %; Table 2).

Diffusive CH<sub>4</sub> flux varied significantly among the four vegetation types sampled in this study (two-way ANOVA with vegetation, season, and their interaction,  $F_{7,979} = 13.2$ ,

**Figure 2.** Net diffusive (a) methane (CH<sub>4</sub>) and (b) nitrous oxide (N<sub>2</sub>O) fluxes by vegetation type. Error bars denote standard errors.

$P < 0.0001$ ; Fig. 2a). However, the effect of vegetation was relatively weak (see ANCOVA results in Section 3.3), and a means comparison test on the pooled data was unable to determine which means differed significantly from the others (Fisher's LSD,  $P > 0.05$ ). For the pooled

data, the overall numerical trend was that mixed palm swamp showed the highest mean flux ( $52.0 \pm 16.0 \text{ mg CH}_4\text{-C m}^{-2} \text{ day}^{-1}$ ), followed by *M. flexuosa* palm swamp ( $36.7 \pm 3.9 \text{ mg CH}_4\text{-C m}^{-2} \text{ day}^{-1}$ ), forested (short pole) vegetation ( $31.6 \pm 6.6 \text{ mg CH}_4\text{-C m}^{-2} \text{ day}^{-1}$ ), and forested vegetation ( $29.8 \pm 10.0 \text{ mg CH}_4\text{-C m}^{-2} \text{ day}^{-1}$ ).  $\text{CH}_4$  ebullition (i.e., net ebullition and ebullition-driven uptake) did not vary significantly among vegetation types or between seasons (Table 2). Broadly speaking, however, we saw a greater frequency of ebullition in the *M. flexuosa* palm swamp, followed by mixed palm swamp, forested vegetation, and forested short pole vegetation (Table 2).

These study sites were also a weak net source of  $\text{N}_2\text{O}$ , with a mean diffusive flux of  $0.70 \pm 0.34 \mu\text{g N}_2\text{O-N m}^{-2} \text{ day}^{-1}$ . We saw only limited evidence of ebullition of  $\text{N}_2\text{O}$ , with only three chambers out of 1181 (0.3% of observations) showing evidence of  $\text{N}_2\text{O}$  ebullition. These data were omitted from the analysis of diffusive flux of  $\text{N}_2\text{O}$ . Because of the high variance in diffusive  $\text{N}_2\text{O}$  flux among plots, analysis of variance indicated that mean diffusive  $\text{N}_2\text{O}$  flux did not differ significantly among vegetation types (two-way ANOVA,  $P > 0.5$ , Fig. 2b). However, when the  $\text{N}_2\text{O}$  flux data were grouped by vegetation type, we see that some vegetation types tended to function as net atmospheric sources, while others acted as atmospheric sinks (Fig. 2b, Table 3). For example, the highest  $\text{N}_2\text{O}$  emissions were observed from *M. flexuosa* palm swamp ( $1.11 \pm 0.44 \mu\text{g N}_2\text{O-N m}^{-2} \text{ day}^{-1}$ ) and forested vegetation ( $0.20 \pm 0.95 \mu\text{g N}_2\text{O-N m}^{-2} \text{ day}^{-1}$ ). In contrast, forested (short pole) vegetation and mixed palm swamp were weak sinks for  $\text{N}_2\text{O}$ , with a mean flux of  $-0.01 \pm 0.84$  and  $-0.21 \pm 0.70 \mu\text{g N}_2\text{O-N m}^{-2} \text{ day}^{-1}$ , respectively.

Soil pH varied significantly among vegetation types (data pooled across all seasons; ANOVA,  $P < 0.0001$ , Table 3). Multiple comparison tests indicated that mean soil pH was significantly different for each of the vegetation types (Fisher's LSD,  $P < 0.0001$ , Table 3), with the lowest pH in forested (short pole) vegetation ( $4.10 \pm 0.04$ ), followed by *M. flexuosa* palm swamp ( $5.32 \pm 0.02$ ), forested vegetation ( $6.15 \pm 0.06$ ), and the mixed palm swamp ( $6.58 \pm 0.04$ ).

Soil DO content varied significantly among vegetation types (data pooled across all seasons; Kruskal–Wallis,  $P < 0.0001$ , Table 3). Multiple comparison tests indicated that mean DO was significantly different for each of the vegetation types (Fisher's LSD,  $P < 0.05$ , Table 3), with the highest DO in the forested (short pole) vegetation ( $25.2 \pm 2.1 \%$ ), followed by the *M. flexuosa* palm swamp ( $18.1 \pm 1.0 \%$ ), forested vegetation ( $11.8 \pm 2.8 \%$ ), and the mixed palm swamp ( $0.0 \pm 0.0 \%$ ).

EC varied significantly among vegetation types (data pooled across all seasons; Kruskal–Wallis,  $P < 0.0001$ , Table 3). Multiple comparison tests indicated that mean EC was significantly different for each of the vegetation types (Fisher's LSD,  $P < 0.05$ ; Table 3), with the highest EC in the mixed palm swamp ( $170.9 \pm 6.0 \mu\text{S m}^{-2}$ ), followed by

**Table 3.** Environmental variables for each vegetation type for the wet and dry season. Values reported here are means and standard errors. Lowercase letters indicate significant differences among vegetation types within the wet or dry season (Fisher's LSD,  $P < 0.05$ ).

Vegetation type	Peat temperature (°C)		Air temperature (°C)		Conductivity ( $\mu\text{S m}^{-2}$ )		Dissolved oxygen (%)		Water table level (cm)		pH	
	Wet season	Dry season	Wet season	Dry season	Wet season	Dry season	Wet season	Dry season	Wet season	Dry season	Wet season	Dry season
Forested	26.1 ± 0.1a	24.7 ± 0.0a	28.8 ± 0.7a	26.4 ± 0.3a	79.0 ± 5.9a	75.9 ± 5.7a	0.2 ± 0.1a	18.9 ± 4.4a	110.8 ± 9.3a	-13.2 ± 0.7a	5.88 ± 0.15a	6.31 ± 0.04a
Forested (short pole)	25.2 ± 0.0b	24.8 ± 0.1a	27.6 ± 0.1b	27.5 ± 0.1b	21.0 ± 0.0b	48.5 ± 4.8b	4.4 ± 0.0a	33.1 ± 2.6b	26.9 ± 0.5b	-4.7 ± 0.4b	4.88 ± 0.01b	3.8 ± 0.03b
<i>M. flexuosa</i> palm swamp	25.6 ± 0.6c	25.3 ± 0.1b	26.3 ± 0.1c	26.4 ± 0.1a	45.9 ± 2.1c	51.9 ± 1.8b	19.4 ± 1.3b	17.3 ± 1.5a	37.2 ± 1.7c	6.1 ± 1.3c	5.04 ± 0.03c	5.49 ± 0.03c
Mixed palm swamp	26.0 ± 0.0a	25.0 ± 0.1ab	26.1 ± 0.1c	28.2 ± 0.3b	100.0 ± 0.2d	206.4 ± 4.2c	0.0 ± 0.0a	0.0 ± 0.0c	183.7 ± 1.7d	-2.4 ± 0.3b	6.1 ± 0.03a	6.82 ± 0.02d

**Table 4.** Trace gas fluxes for each vegetation type for the wet and dry season. Values reported here are means and standard errors. Uppercase letters indicate significant differences in gas flux between seasons within a vegetation type, while lowercase letters indicate significant differences among vegetation types within a season (Fisher's LSD,  $P < 0.05$ ).

Vegetation type	Methane flux (mg CH <sub>4</sub> -C m <sup>-2</sup> day <sup>-1</sup> )		Nitrous oxide flux (µg N <sub>2</sub> O-N m <sup>-2</sup> day <sup>-1</sup> )	
	Wet season	Dry season	Wet season	Dry season
Forested	6.7 ± 1.0Aa	47.2 ± 5.4Ba	2.54 ± 1.48	-1.16 ± 1.20
Forested (short pole)	60.4 ± 9.1Ab	18.8 ± 2.6Bb	1.16 ± 0.54	-0.42 ± 0.90
<i>M. flexuosa</i> palm swamp	46.7 ± 8.4Ac	28.3 ± 2.6Bc	1.14 ± 0.35	0.92 ± 0.61
Mixed palm swamp	6.1 ± 1.3Aa	64.2 ± 12.1Ba	1.45 ± 0.79	-0.80 ± 0.79

forested vegetation ( $77.1 \pm 4.2 \mu\text{S m}^{-2}$ ), *M. flexuosa* palm swamp ( $49.7 \pm 1.4 \mu\text{S m}^{-2}$ ), and the forested (short pole) vegetation ( $40.9 \pm 3.5 \mu\text{S m}^{-2}$ ).

Soil temperature varied significantly among vegetation types (data pooled across all seasons; ANOVA,  $P < 0.0001$ , Table 3). Multiple comparison tests indicated that soil temperature in forested (short pole) vegetation was significantly lower than in the other vegetation types (Table 3), whereas the other vegetation types did not differ in temperature amongst themselves (Fisher's LSD,  $P < 0.05$ , Table 3).

Air temperature varied significantly among vegetation types (data pooled across all seasons; ANOVA,  $P < 0.0001$ , Table 3). Multiple comparison tests indicated that air temperature in *M. flexuosa* palm swamp was significantly lower than in the other vegetation types, whereas the other vegetation types did not differ in temperature amongst themselves (Fisher's LSD,  $P < 0.05$ , Table 3).

Water table depths varied significantly among vegetation types (data pooled across all seasons; ANOVA,  $P < 0.0001$ , Table 3). The highest mean water tables were observed in mixed palm swamp ( $59.6 \pm 9.3$  cm), followed by forested vegetation ( $34.0 \pm 6.9$  cm), *M. flexuosa* palm swamp ( $17.4 \pm 1.2$  cm), and forested (short pole) vegetation ( $3.5 \pm 1.0$  cm) (Fisher's LSD,  $P < 0.0005$ ).

### 3.2 Temporal variations in gas fluxes and environmental variables

The peatlands sampled in this study showed pronounced seasonal variability in diffusive CH<sub>4</sub> flux (two-way ANOVA,  $F_{7,979} = 13.2$ ,  $P < 0.0001$ ; Table 4). For ebullition of CH<sub>4</sub> and ebullition-driven uptake of CH<sub>4</sub>, mean fluxes varied between seasons, but high variability meant that these differences were not statistically significant (two-way ANOVA,  $P > 0.8$ ; Table 2). Diffusive N<sub>2</sub>O flux showed no seasonal trends (two-way ANOVA,  $P > 0.5$ ) and therefore will not be discussed further here. Diurnal studies suggest that diffusive fluxes of neither CH<sub>4</sub> nor N<sub>2</sub>O varied over the course of a 24 h period.

For diffusive CH<sub>4</sub> flux, the overall trend was towards significantly higher wet season ( $51.1 \pm 7.0$  mg CH<sub>4</sub>-

C m<sup>-2</sup> day<sup>-1</sup>) compared to dry season ( $27.3 \pm 2.7$  mg CH<sub>4</sub>-C m<sup>-2</sup> day<sup>-1</sup>) flux (data pooled across all vegetation types;  $t$  test,  $P < 0.001$ , Table 4). However, when diffusive CH<sub>4</sub> flux was disaggregated by vegetation type, very different seasonal trends emerged. For example, both forested vegetation and mixed palm swamp showed significantly greater diffusive CH<sub>4</sub> flux during the *dry season* with net fluxes of  $47.2 \pm 5.4$  and  $64.2 \pm 12.1$  mg CH<sub>4</sub>-C m<sup>-2</sup> day<sup>-1</sup>, respectively (Fisher's LSD,  $P < 0.05$ , Table 3). In contrast, *wet season* flux was 7–16 times lower, with net fluxes of  $6.7 \pm 1.0$  and  $6.1$  mg CH<sub>4</sub>-C m<sup>-2</sup> day<sup>-1</sup>, respectively (Fisher's LSD,  $P < 0.05$ , Table 3). In contrast, forested (short pole) vegetation and *M. flexuosa* palm swamp showed seasonal trends consistent with the pooled dataset, i.e., significantly higher flux during the wet season ( $46.7 \pm 8.4$  and  $60.4 \pm 9.1$  mg CH<sub>4</sub>-C m<sup>-2</sup> day<sup>-1</sup>, respectively) compared to the dry season ( $28.3 \pm 2.6$  and  $18.8 \pm 2.6$  mg CH<sub>4</sub>-C m<sup>-2</sup> day<sup>-1</sup>, respectively) (Fisher's LSD,  $P < 0.05$ , Table 3).

Even though seasonal trends in CH<sub>4</sub> ebullition were not statistically significant, we will briefly describe the overall patterns for the different vegetation types as they varied among ecosystems (Table 2). Forested vegetation only showed evidence of ebullition during the dry season, where ebullition-driven uptake was observed. For forested (short pole) vegetation, net ebullition was generally greater during the wet season, while ebullition-driven uptake was higher during the dry season. For *M. flexuosa* palm swamp, both net ebullition and ebullition-driven uptake were greater during the wet season. Lastly, for mixed palm swamp, both net ebullition and ebullition-driven uptake were greater during the dry season.

For the environmental variables, soil pH, DO, EC, water table depth, and soil temperature varied significantly between seasons, whereas air temperature did not. Thus, for sake of brevity, air temperature is not discussed further here. Mean soil pH was significantly lower during the wet season ( $5.18 \pm 0.03$ ) than during the dry season ( $5.31 \pm 0.04$ ) (data pooled across all vegetation types;  $t$  test,  $P < 0.05$ , Table 2). When disaggregated by vegetation type, the overall trend was found to hold true for all vegetation types except forested



(short pole) vegetation, which displayed higher pH during the wet season compared to the dry season (Table 2). A two-way ANOVA on Box–Cox transformed data using vegetation type, season, and their interaction as explanatory variables indicated that vegetation type was the best predictor of pH, with season and vegetation type by season playing a lesser role ( $F_{7,1166} = 348.9$ ,  $P < 0.0001$ ).

For DO, the overall trend was towards significantly lower DO during the wet season ( $13.9 \pm 1.0\%$ ) compared to the dry season ( $19.3 \pm 1.2\%$ ) (data pooled across all vegetation types; Wilcoxon test,  $P < 0.0001$ , Table 2). However, when the data were disaggregated by vegetation type, we found that individual vegetation types showed distinct seasonal trends from each other. Forested vegetation and mixed palm swamp were consistent with the overall trend (i.e., lower wet season compared to dry season DO), whereas forested (short pole) vegetation and *M. flexuosa* palm swamp displayed the reverse trend (i.e., higher wet season compared to dry season DO) (Table 2). A two-way ANOVA on Box–Cox transformed data using vegetation type, season, and their interaction as explanatory variables indicated that vegetation type was the best predictor of DO, followed by a strong vegetation by season interaction; season itself played a lesser role than either of the other two explanatory variables ( $F_{7,1166} = 57.0$ ,  $P < 0.0001$ ).

For EC, the overall trend was towards lower EC in the wet season ( $49.4 \pm 1.8 \mu\text{S m}^{-2}$ ) compared to the dry season ( $65.5 \pm 2.2 \mu\text{S m}^{-2}$ ) (data pooled across all vegetation types; Wilcoxon test,  $P < 0.05$ , Table 2). When the data were disaggregated by vegetation type, this trend was consistent for all the vegetation types except for forested vegetation, where differences between wet and dry season were not statistically significant (Wilcoxon,  $P > 0.05$ , Table 2).

Water table depths varied significantly between seasons (data pooled across all vegetation types; Wilcoxon test,  $P < 0.0001$ , Table 2). Mean water table level was significantly higher in the wet ( $54.1 \pm 2.7$  cm) than the dry ( $1.3 \pm 0.8$  cm) season. When disaggregated by vegetation type, the trend held true for individual vegetation types (Table 2). All vegetation types had negative dry season water tables (i.e., below the soil surface) and positive wet season water tables (i.e., water table above the soil surface), except for *M. flexuosa* palm swamp that had positive water tables in both seasons. Two-way ANOVA on Box–Cox transformed data using vegetation type, season, and their interaction as explanatory variables indicated that all three factors explained water table depth, but that season accounted for the largest proportion of the variance in the model, followed by vegetation by season and lastly by vegetation type ( $F_{7,1157} = 440.1$ ,  $P < 0.0001$ ).

For soil temperature, the overall trend was towards slightly higher temperatures in the wet season ( $25.6 \pm 0.0^\circ\text{C}$ ) compared to the dry season ( $25.1 \pm 0.0^\circ\text{C}$ ) ( $t$  test,  $P < 0.0001$ ). Analysis of the disaggregated data indicates this trend was consistent for individual vegetation types (Table 2). Two-

way ANOVA on Box–Cox transformed data using vegetation type, season, and their interaction as explanatory variables indicated that all three variables played a significant role in modulating soil temperature, although season accounted for the largest proportion of the variance whereas the other two factors accounted for a similar proportion of the variance ( $F_{7,1166} = 21.3$ ,  $P < 0.0001$ ).

### 3.3 Relationships between gas fluxes and environmental variables

To explore the relationships between environmental variables and diffusive gas fluxes, we conducted an ANCOVA on Box–Cox transformed gas flux data, using vegetation type, season, vegetation by season, and environmental variables as explanatory variables. We did not analyze trends between ebullition and environmental variables because of the limitations in the sampling methodology and the limited number of observations.

For diffusive  $\text{CH}_4$  flux, ANCOVA revealed that vegetation by season was the strongest predictor of  $\text{CH}_4$  flux, followed by a strong season effect ( $F_{13,917} = 9.2$ ,  $P < 0.0001$ ). Other significant drivers included soil temperature, water table depth, and a borderline-significant effect of vegetation type ( $P < 0.06$ ). However, it is important to note that each of these environmental variables was only weakly correlated with  $\text{CH}_4$  flux even when the relationships were statistically significant; for example, when individual bivariate regressions were calculated, the  $r^2$  values were less than 0.01 for each plot (see Figs. S1 and S2 in the Supplement).

For diffusive  $\text{N}_2\text{O}$  flux, ANCOVA indicated that the best predictors of flux rates were dissolved oxygen and electrical conductivity ( $F_{13,1014} = 2.2$ ,  $P < 0.0082$ ). As was the case for  $\text{CH}_4$ , when the relationships between these environmental variables and  $\text{N}_2\text{O}$  flux were explored using individual bivariate regressions,  $r^2$  values were found to be very low (e.g., less than  $r^2 < 0.0007$ ) or not statistically significant (see Figs. S3 and S4).

## 4 Discussion

### 4.1 Large and asynchronous $\text{CH}_4$ fluxes from peatlands in the Pastaza–Marañón foreland basin

The ecosystems sampled in this study were strong atmospheric sources of  $\text{CH}_4$ . Diffusive  $\text{CH}_4$  flux, averaged across all vegetation types, was  $36.1 \pm 3.1 \text{ mg CH}_4\text{-C m}^{-2} \text{ day}^{-1}$ , spanning a range from  $-100$  to  $1510 \text{ mg CH}_4\text{-C m}^{-2} \text{ day}^{-1}$ . This mean falls within the range of other diffusive fluxes observed in Indonesian peatlands ( $3.7\text{--}87.8 \text{ mg CH}_4\text{-C m}^{-2} \text{ day}^{-1}$ ) (Couwenberg et al., 2010) and other Amazonian wetlands ( $7.1\text{--}390.0 \text{ mg CH}_4\text{-C m}^{-2} \text{ day}^{-1}$ ) (Bartlett et al., 1988, 1990; Devol et al., 1988, 1990). Although the ebullition data must be treated with caution because of the sampling methodology (see below), we observed a mean

net ebullition flux of  $973.3 \pm 161.4 \text{ mg CH}_4\text{-C m}^{-2} \text{ day}^{-1}$ , spanning a range of 27 to  $8082 \text{ mg CH}_4\text{-C m}^{-2} \text{ day}^{-1}$ . While data on ebullition from Amazonian wetlands are sparse, these values are broadly in line with riverine and lake ecosystems sampled elsewhere (Bastviken et al., 2010; Smith et al., 2000; Sawakuchi et al., 2014). Ebullition-driven  $\text{CH}_4$  uptake is not a commonly reported phenomena in other peatland studies because it is likely an artefact of chamber sampling methods; as a consequence, we do not discuss these data further here. To summarize, these data on diffusive  $\text{CH}_4$  flux and ebullition suggest that peatlands in the Pastaza–Marañón foreland basin are strong contributors to the regional atmospheric budget of  $\text{CH}_4$ , given that the four vegetation types sampled here represent the dominant cover types in the PMFB (Draper et al., 2014; Householder et al., 2012; Kelly et al., 2014; Lahteenoja and Page, 2011)

The overall trend in the diffusive flux data was towards greater temporal (i.e., seasonal) variability in diffusive  $\text{CH}_4$  flux rather than strong spatial (i.e., inter-site) variability. For the pooled dataset, diffusive  $\text{CH}_4$  emissions were significantly greater during the wet season than the dry season, with emissions falling by approximately half from one season to the other (i.e.,  $51.1 \pm 7.0$  to  $27.3 \pm 2.7 \text{ mg CH}_4\text{-C m}^{-2} \text{ day}^{-1}$ ). This is in contrast to the data on diffusive  $\text{CH}_4$  flux among study sites, where statistical analyses indicate that there was a weak effect of vegetation type on  $\text{CH}_4$  flux, that was only on the edge of statistical significance (i.e., ANCOVA;  $P < 0.06$  for the vegetation effect term). For the ebullition data, while there was no significant difference among vegetation types or between seasons, it is interesting to note that ebullition was more common for the two vegetation types – mixed palm swamp and *M. flexuosa* palm swamp – that showed the highest rates of diffusive  $\text{CH}_4$  flux (Fig. 2, Table 2). In contrast, forested and forested (short pole) vegetation, which showed the lowest rates of diffusive  $\text{CH}_4$  flux, also showed the lowest occurrence of ebullition (Fig. 2, Table 2). This is broadly consistent with the notion that mixed palm swamp and *M. flexuosa* palm swamp may produce more  $\text{CH}_4$  or possess lower gross  $\text{CH}_4$  oxidation rates than the other vegetation types.

At face value, these data on diffusive  $\text{CH}_4$  flux suggest two findings: first, the relatively weak effect of vegetation type on diffusive  $\text{CH}_4$  flux implies that patterns of  $\text{CH}_4$  cycling are broadly similar among study sites. Second, the strong overall seasonal pattern suggests that – on the whole – these systems conform to our normative expectations of how peatlands function with respect to seasonal variations in hydrology and redox potential, i.e., enhanced  $\text{CH}_4$  emissions during a more anoxic wet season (i.e., when water tables rise) and reduced  $\text{CH}_4$  emissions during a more oxic dry season (i.e., when water tables fall). However, closer inspection of the data reveals that different vegetation types showed contrasting seasonal emission patterns (Table 3), challenging our basic assumptions about how these ecosystems function. For example, while forested (short pole) vegetation and

*M. flexuosa* palm swamp conformed to expected seasonal trends for methanogenic wetlands (i.e., higher wet season compared to dry season emissions), forested vegetation and mixed palm swamp showed the opposite pattern, with significantly greater  $\text{CH}_4$  emissions during the dry season. The disaggregated data thus imply that the process-based controls on  $\text{CH}_4$  fluxes may vary significantly among these different ecosystems, rather than being similar, leading to a divergence in seasonal flux patterns.

What may explain this pattern of seasonal divergence in  $\text{CH}_4$  flux? One explanation is that  $\text{CH}_4$  emissions from forested vegetation and mixed palm swamp, compared to the other two ecosystems, may be more strongly transport-limited during the wet season than the dry season. This interpretation is supported by the field data; forested vegetation and mixed palm swamp had the highest wet season water table levels, measuring  $110.8 \pm 9.3$  and  $183.7 \pm 1.7 \text{ cm}$ , respectively (Table 2). In contrast, water table levels for forested (short pole) vegetation and *M. flexuosa* palm swamp in the wet season were 3–7 times lower, measuring only  $26.9 \pm 0.5$  and  $37.2 \pm 1.7 \text{ cm}$ , respectively (Table 2). Moreover, a scatter plot of diffusive  $\text{CH}_4$  flux against water table depth shows a peak in diffusive  $\text{CH}_4$  emissions when water tables are between 30 and 40 cm above the surface, after which  $\text{CH}_4$  emissions decline precipitously (Fig. S2). Thus, the greater depth of overlying water in forested vegetation and mixed palm swamp may have exerted a much greater physical constraint on gas transport compared to the other two ecosystems. This interpretation is broadly consistent with studies from other ecosystems, which indicate that high or positive water tables may suppress  $\text{CH}_4$  emissions from wetlands above a system-specific threshold (Couwenberg et al., 2010, 2011).

However, transport limitation alone does not fully explain the difference in dry season  $\text{CH}_4$  emissions among vegetation types. Forested vegetation and mixed palm swamp showed substantially higher dry season  $\text{CH}_4$  emissions ( $47.2 \pm 5.4$  and  $85.5 \pm 26.4 \text{ mg CH}_4\text{-C m}^{-2} \text{ day}^{-1}$ , respectively) compared to forested (short pole) vegetation and *M. flexuosa* palm swamp ( $9.6 \pm 2.6$  and  $25.5 \pm 2.9 \text{ mg CH}_4\text{-C m}^{-2} \text{ day}^{-1}$ , respectively), pointing to underlying differences in  $\text{CH}_4$  production and oxidation among these ecosystems. One possibility is that dry season methanogenesis in forested vegetation and mixed palm swamp was greater than in the other two ecosystems, potentially driven by higher rates of C flow (Whiting and Chanton, 1993). This is plausible given that forested vegetation and mixed palm swamp tend to occur in more nutrient-rich parts of the Pastaza–Marañón foreland basin, whereas forested (short pole) vegetation and *M. flexuosa* palm swamp tend to dominate in more nutrient-poor areas (Lahteenoja et al., 2009a), leading to potential differences in rates of plant productivity and below-ground C flow. Moreover, it is possible that the nutrient-rich vegetation may be able to utilize the higher concentration of nutrients, deposited during the flood pulse, during the Ama-

zonian dry season (Morton et al., 2014; Saleska et al., 2016), with implications for overall ecosystem C throughput and CH<sub>4</sub> emissions. Of course, this interpretation does not preclude other explanations, such as differences in CH<sub>4</sub> transport rates among ecosystems (e.g., due to plant-facilitated transport or ebullition) (Panagala et al., 2013) or varying rates of CH<sub>4</sub> oxidation (Teh et al., 2005). However, these other possibilities cannot be explored further without recourse to more detailed process-level experiments. Forthcoming studies on the regulation of GHG fluxes at finer spatial scales (e.g., investigation of environmental gradients within individual study sites) or detailed diurnal studies of GHG exchange (Murphy et al., 2017) will further deepen our understanding of the process controls on soil GHG flux from these peatlands and shed light on these questions.

Finally, while the trends described here are intriguing, it is important to acknowledge some of the potential limitations of our data. First, given the uneven sampling pattern, it is possible that the values reported here do not fully represent the entire range of diffusive flux rates, especially for the more sparsely sampled habitats. However, given the large and statistically significant differences in CH<sub>4</sub> emissions between seasons, it is likely that the main trends that we have identified will hold true with more spatially extensive sampling. Second, the data are a conservative underestimate of CH<sub>4</sub> emissions, because the low-frequency, static chamber sampling approach that we utilized was unable to fully capture erratic ebullition events representatively (McClain et al., 2003). Although we attempted to quantify CH<sub>4</sub> ebullition within our static flux chambers, the sampling approach that we utilized was not the best suited for representatively quantifying ebullition. Given the erratic or stochastic nature of ebullition, automated chamber measurements or an inverted “flux funnel” approach would have provided better estimates of ebullition (Strack et al., 2005). However, we lacked the resources to apply these techniques here. We also did not measure CH<sub>4</sub> emissions from the stems of woody plants, even though woody plants have been recently identified as an important point of atmospheric egress (Pangala et al., 2013). We did not have enough data on floristic composition or individual plant identities within our plots to develop a sampling design that would adequately represent plant-mediated fluxes from our study sites or the resources to implement a separate study of stem fluxes. Third and last, our data probably underestimate net CH<sub>4</sub> fluxes for the PMFB because we chose to include fluxes with strong negative values (i.e., more than  $-10 \text{ mg CH}_4\text{-C m}^{-2} \text{ day}^{-1}$ ) in our calculation of mean diffusive flux rates. These observations are more negative than other values typically reported elsewhere in the tropical wetland literature (Bartlett et al., 1988, 1990; Devol et al., 1988, 1990; Couwenberg et al., 2010). However, they represent only a small proportion of our dataset (i.e., 7%, or only 68 out of 980 measurements), and inspection of our field notes and the data itself did not produce convincing reasons to exclude these observations (e.g., we found no evi-

dence of irregularities during field sampling, and any chambers that showed statistically insignificant changes in concentration over time were removed during our quality control procedures). While headspace concentrations for these measurements were often elevated above mean tropospheric levels ( $> 2 \text{ ppm}$ ), this in itself is not unusual in reducing environments that contain strong local sources of CH<sub>4</sub> (Baldocchi et al., 2012). We did not see this as a reason to omit these values as local concentrations of CH<sub>4</sub> are likely to vary naturally in methanogenic forest environments due to poor mixing in the understory and episodic ebullition events. Importantly, exclusion of these data did not alter the overall statistical trends reported above and only produced slightly higher estimates of diffusive CH<sub>4</sub> flux ( $41.6 \pm 3.2 \text{ mg CH}_4\text{-C m}^{-2} \text{ day}^{-1}$  vs.  $36.1 \pm 3.1 \text{ mg CH}_4\text{-C m}^{-2} \text{ day}^{-1}$ ).

#### 4.2 Western Amazonian peatlands as weak atmospheric sources of nitrous oxide

The ecosystems sampled in this study were negligible atmospheric sources of N<sub>2</sub>O, emitting only  $0.70 \pm 0.34 \mu\text{g N}_2\text{O-N m}^{-2} \text{ day}^{-1}$ , suggesting that peatlands in the Pastaza–Marañón foreland basin make little or no contribution to regional atmospheric budgets of N<sub>2</sub>O. This is consistent with N<sub>2</sub>O flux measurements from other forested tropical peatlands, where N<sub>2</sub>O emissions were also found to be relatively low (Inubushi et al., 2003; Couwenberg et al., 2010). No statistically significant differences in N<sub>2</sub>O flux were observed among study sites or between seasons, suggesting that these different peatlands may have similar patterns of N<sub>2</sub>O cycling. Interestingly, differences in N<sub>2</sub>O fluxes were not associated with the nutrient status of the peatland; i.e., more nutrient-rich ecosystems, such as forested vegetation and mixed palm swamp, did not show higher N<sub>2</sub>O fluxes than their nutrient-poor counterparts, such as forested (short pole) vegetation and *M. flexuosa* palm swamp. This may imply that N availability, one of the principal drivers of nitrification, denitrification, and N<sub>2</sub>O production (Groffman et al., 2009; Werner et al., 2007), may not be greater in nutrient-rich versus nutrient-poor ecosystems in this part of the western Amazon. Alternatively, it is possible that even though N availability and N fluxes may differ between nutrient-rich and nutrient-poor systems, N<sub>2</sub>O yield may also vary such that net N<sub>2</sub>O emissions are not significantly different among study sites (Teh et al., 2014).

One potential source of concern are the negative N<sub>2</sub>O fluxes that we documented here. While some investigators have attributed negative fluxes to instrumental error (Cowan et al., 2014; Chapuis-Lardy et al., 2007), others have demonstrated that N<sub>2</sub>O consumption – particularly in wetland soils – is not an experimental artifact but occurs due to the complex effects of redox, organic carbon content, nitrate availability, and soil transport processes on denitrification (Ye and Horwath, 2016; Yang et al., 2011; Wen et al., 2016; Schlesinger, 2013; Teh et al., 2014; Chapuis-Lardy et al.,

2007). Given the low redox potential and high carbon content of these soils, it is plausible that microbial N<sub>2</sub>O consumption is occurring, because these types of conditions have been found to be conducive for N<sub>2</sub>O uptake elsewhere (Ye and Horwath, 2016; Teh et al., 2014; Yang et al., 2011).

## 5 Conclusions

Our data suggest that peatlands in the Pastaza–Marañón foreland basin are strong sources of atmospheric CH<sub>4</sub> at a regional scale and need to be better accounted for in CH<sub>4</sub> emissions inventories for the Amazon basin as a whole. In contrast, N<sub>2</sub>O fluxes were negligible, suggesting that these ecosystems are weak regional sources at best. Divergent or asynchronous seasonal emissions patterns for CH<sub>4</sub> among different vegetation types were intriguing and challenge our underlying expectations of how tropical peatlands function. These data highlight the need for greater wet season sampling, particularly from ecosystems near river margins that may experience very high water tables (i.e., > 40 cm). Moreover, these data also emphasize the need for more spatially extensive sampling across both the Pastaza–Marañón foreland basin and the wider Amazon region as a whole in order to establish if these asynchronous seasonal emission patterns are commonplace or specific to peatlands in the PMFB region. If CH<sub>4</sub> emission patterns for different peatlands in the Amazon are in fact asynchronous and decoupled from rainfall seasonality, then this may partially explain some of the heterogeneity in CH<sub>4</sub> sources and sinks observed at the basin-wide scale (Wilson et al., 2016).

*Data availability.* These data are publicly available through the UK Natural Environment Research Council's (NERC) Centre for Environmental Data Analysis (CEDA), with DOI <http://dx.doi.org/10.5072/a3614fb00ff74999a5187d3a3767d96d>.

**The Supplement related to this article is available online at <https://doi.org/10.5194/bg-14-3669-2017-supplement>.**

*Author contributions.* Yit Arn Teh secured the funding for this research, assisted in the planning and design of the experiment, and took the principal role in the analysis of the data and preparation of the manuscript. Wayne A. Murphy planned and designed the experiment, collected the field data, analyzed the samples, and took a secondary role in data preparation, data analysis, and manuscript preparation. Juan-Carlos Berrio, Arnoud Boom, and Susan E. Page supported the planning and design of the experiment and provided substantive input into the writing of the manuscript. Arnoud Boom in particular took a lead role in developing the maps of our study sites in the PMFB.

*Competing interests.* The authors declare that they have no conflict of interest.

*Acknowledgements.* The authors would like to acknowledge the UK Natural Environment Research Council for funding this research (NERC award number NE/I015469). We would like to thank MINAG and the Ministerio de Turismo in Iquitos for permits to conduct this research; the Instituto de Investigaciones de la Amazonía Peruana (IIAP) for logistical support; Peruvian rainforest villagers for their warm welcome and acceptance; Hugo Vasquez, Pierro Vasquez, Gian Carlo Padilla Tenazoa, and Yully Rojas Reátegui for fieldwork assistance; Outi Lahteenoja and Ethan Householder for fieldwork planning; and Paul Beaver of Amazonia Expeditions for lodging and logistical support. Our gratitude also goes to Alex Cumming for fieldwork support and laboratory assistance and Bill Hickin, Gemma Black, Adam Cox, Charlotte Langley, Kerry Allen, and Lisa Barber of the University of Leicester for all of their continued support. Thanks are also owed to Graham Hambley (St Andrews), Angus Calder (St Andrews), Viktoria Oliver (Aberdeen), Torsten Diem (Aberdeen), Tom Kelly (Leeds), and Freddie Draper (Leeds) for their help in the laboratory and with fieldwork planning. Torsten Diem, Viktoria Oliver, and two anonymous referees provided very helpful and constructive comments on earlier drafts of this paper. This publication is a contribution from the Scottish Alliance for Geoscience, Environment and Society (<http://www.sages.ac.uk>) and the UK Tropical Peatland Working Group (<https://tropicalpeat.wordpress.com>).

Edited by: Ivonne Trebs

Reviewed by: Edzo Veldkamp and one anonymous referee

## References

- Andriessse, J.: Nature and management of tropical peat soils, Food & Agriculture Org., Rome, Italy, 45–59, 1988.
- Baggs, E. M.: A review of stable isotope techniques for N<sub>2</sub>O source partitioning in soils: Recent progress, remaining challenges and future considerations, *Rapid Commun. Mass Spectrom.*, 22, 1664–1672, 2008.
- Baldocchi, D., Detto, M., Sonnentag, O., Verfaillie, J., Teh, Y. A., Silver, W., and Kelly, N. M.: The challenges of measuring methane fluxes and concentrations over a peatland pasture, *Agr. Forest Meteorol.*, 153, 177–187, <https://doi.org/10.1016/j.agrformet.2011.04.013>, 2012.
- Bartlett, K. B., Crill, P. M., Sebacher, D. I., Harriss, R. C., Wilson, J. O., and Melack, J. M.: Methane flux from the Central Amazonian floodplain, *J. Geophys. Res.-Atmos.*, 93, 1571–1582, 1988.
- Bartlett, K. B., Crill, P. M., Bonassi, J. A., Richey, J. E., and Harriss, R. C.: Methane flux from the Amazon River floodplain - emissions during rising water, *J. Geophys. Res.-Atmos.*, 95, 16773–16788, <https://doi.org/10.1029/JD095iD10p16773>, 1990.
- Bastviken, D., Santoro, A. L., Marotta, H., Pinho, L. Q., Calheiros, D. F., Crill, P., and Enrich-Prast, A.: Methane Emissions from Pantanal, South America, during the Low Water Season: Toward More Comprehensive Sampling, *Environ. Sci. Technol.*, 44, 5450–5455, <https://doi.org/10.1021/es1005048>, 2010.

- Belyea, L. R. and Baird, A. J.: Beyond “The limits to peat bog growth”: Cross-scale feedback in peatland development, *Ecol. Monogr.*, 76, 299–322, 2006.
- Blazewicz, S. J., Petersen, D. G., Waldrop, M. P., and Firestone, M. K.: Anaerobic oxidation of methane in tropical and boreal soils: Ecological significance in terrestrial methane cycling, *J. Geophys. Res.-Biogeo.*, 117, 1–9, <https://doi.org/10.1029/2011JG001864>, 2012.
- Chapuis-Lardy, L., Wrage, N., Metay, A., Chotte, J.-L., and Bernoux, M.: Soils, a sink for N<sub>2</sub>O? A review, *Global Change Biol.*, 13, 1–17, <https://doi.org/10.1111/j.1365-2486.2006.01280.x>, 2007.
- Conrad, R.: Soil Microorganisms as Controllers of Atmospheric Trace Gases, *Microbiol. Rev.*, 60, 609–640, 1996.
- Couwenberg, J., Dommain, R., and Joosten, H.: Greenhouse gas fluxes from tropical peatlands in south-east Asia, *Global Change Biol.*, 16, 1715–1732, <https://doi.org/10.1111/j.1365-2486.2009.02016.x>, 2010.
- Couwenberg, J., Thiele, A., Tanneberger, F., Augustin, J., Bärtsch, S., Dubovik, D., Liashchynskaya, N., Michaelis, D., Minke, M., Skuratovich, A., and Joosten, H.: Assessing greenhouse gas emissions from peatlands using vegetation as a proxy, *Hydrobiologia*, 674, 67–89, <https://doi.org/10.1007/s10750-011-0729-x>, 2011.
- Cowan, N. J., Famulari, D., Levy, P. E., Anderson, M., Reay, D. S., and Skiba, U. M.: Investigating uptake of N<sub>2</sub>O in agricultural soils using a high-precision dynamic chamber method, *Atmos. Meas. Tech.*, 7, 4455–4462, <https://doi.org/10.5194/amt-7-4455-2014>, 2014.
- D’Amelio, M. T. S., Gatti, L. V., Miller, J. B., and Tans, P.: Regional N<sub>2</sub>O fluxes in Amazonia derived from aircraft vertical profiles, *Atmos. Chem. Phys.*, 9, 8785–8797, <https://doi.org/10.5194/acp-9-8785-2009>, 2009.
- Devol, A. H., Richey, J. E., Clark, W. A., King, S. L., and Martinelli, L. A.: Methane emissions to the troposphere from the Amazon floodplain, *J. Geophys. Res.-Atmos.*, 93, 1583–1592, <https://doi.org/10.1029/JD093iD02p01583>, 1988.
- Devol, A. H., Richey, J. E., Forsberg, B. R., and Martinelli, L. A.: Seasonal dynamics in methane emissions from the Amazon River floodplain to the troposphere, *J. Geophys. Res.-Atmos.*, 95, 16417–16426, <https://doi.org/10.1029/JD095iD10p16417>, 1990.
- Draper, F. C., Roucoux, K. H., Lawson, I. T., Mitchard, E. T. A., Coronado, E. N. H., Lahteenoja, O., Montenegro, L. T., Sandoval, E. V., Zarate, R., and Baker, T. R.: The distribution and amount of carbon in the largest peatland complex in Amazonia, *Environ. Res. Lett.*, 9, 1–12, <https://doi.org/10.1088/1748-9326/9/12/124017>, 2014.
- Espinoza Villar, J. C., Guyot, J. L., Ronchail, J., Cochonneau, G., Filizola, N., Fraizy, P., Labat, D., de Oliveira, E., Ordoñez, J. J., and Vauchel, P.: Contrasting regional discharge evolutions in the Amazon basin (1974–2004), *J. Hydrol.*, 375, 297–311, 2009a.
- Espinoza Villar, J. C., Ronchail, J., Guyot, J. L., Cochonneau, G., Naziano, F., Lavado, W., De Oliveira, E., Pombosa, R., and Vauchel, P.: Spatio-temporal rainfall variability in the Amazon basin countries (Brazil, Peru, Bolivia, Colombia, and Ecuador), *Int. J. Climatol.*, 29, 1574–1594, 2009b.
- Firestone, M. K. and Davidson, E. A.: Microbiological basis of NO and N<sub>2</sub>O production and consumption in soil, in: Exchange of Trace Gases Between Terrestrial Ecosystems and the Atmosphere, edited by: Andrae, M. O. and Schimel, D. S., John Wiley and Sons Ltd., New York, 7–21, 1989.
- Firestone, M. K., Firestone, R. B., and Tiedje, J. M.: Nitrous oxide from soil denitrification: Factors controlling its biological production, *Science*, 208, 749–751, 1980.
- Groffman, P. M., Butterbach-Bahl, K., Fulweiler, R. W., Gold, A. J., Morse, J. L., Stander, E. K., Tague, C., Tonitto, C., and Vidon, P.: Challenges to incorporating spatially and temporally explicit phenomena (hotspots and hot moments) in denitrification models, *Biogeochemistry*, 93, 49–77, <https://doi.org/10.1007/s10533-008-9277-5>, 2009.
- Hanson, R. S. and Hanson, T. E.: Methanotrophic Bacteria, *Microbiol. Rev.*, 60, 439–471, 1996.
- Householder, J. E., Janovec, J., Tobler, M., Page, S., and Lahteenoja, O.: Peatlands of the Madre de Dios River of Peru: Distribution, Geomorphology, and Habitat Diversity, *Wetlands*, 32, 359–368, <https://doi.org/10.1007/s13157-012-0271-2>, 2012.
- Huang, J., Golombek, A., Prinn, R., Weiss, R., Fraser, P., Simmonds, P., Dlugokencky, E. J., Hall, B., Elkins, J., Steele, P., Langenfelds, R., Krummel, P., Dutton, G., and Porter, L.: Estimation of regional emissions of nitrous oxide from 1997 to 2005 using multinetwerk measurements, a chemical transport model, and an inverse method, *J. Geophys. Res.-Atmos.*, 113, D17313, <https://doi.org/10.1029/2007jd009381>, 2008.
- Inubushi, K., Furukawa, Y., Hadi, A., Purnomo, E., and Tsuruta, H.: Seasonal changes of CO<sub>2</sub>, CH<sub>4</sub> and N<sub>2</sub>O fluxes in relation to land-use change in tropical peatlands located in coastal area of South Kalimantan, *Chemosphere*, 52, 603–608, [https://doi.org/10.1016/s0045-6535\(03\)00242-x](https://doi.org/10.1016/s0045-6535(03)00242-x), 2003.
- Jungkunst, H. F. and Fiedler, S.: Latitudinal differentiated water table control of carbon dioxide, methane and nitrous oxide fluxes from hydromorphic soils: feedbacks to climate change, *Global Change Biol.*, 13, 2668–2683, <https://doi.org/10.1111/j.1365-2486.2007.01459.x>, 2007.
- Junk, W.: Flood tolerance and tree distribution in central Amazonian floodplains, in: Tropical forests: Botanical dynamics, speciation and diversity, Academic Press, London, UK, 47–64, 1989.
- Keller, M., Kaplan, W. A., and Wofsy, S. C.: Emissions of N<sub>2</sub>O, CH<sub>4</sub> and CO<sub>2</sub> from tropical forest soils, *J. Geophys. Res.-Atmos.*, 91, 1791–1802, <https://doi.org/10.1029/JD091iD11p1791>, 1986.
- Kelly, T. J., Baird, A. J., Roucoux, K. H., Baker, T. R., Honorio Coronado, E. N., Ríos, M., and Lawson, I. T.: The high hydraulic conductivity of three wooded tropical peat swamps in northeast Peru: measurements and implications for hydrological function, *Hydrol. Process.*, 28, 3373–3387, <https://doi.org/10.1002/hyp.9884>, 2014.
- Kirschke, S., Bousquet, P., Ciais, P., Saunois, M., Canadell, J. G., Dlugokencky, E. J., Bergamaschi, P., Bergmann, D., Blake, D. R., Bruhwiler, L., Cameron-Smith, P., Castaldi, S., Chevallier, F., Feng, L., Fraser, A., Heimann, M., Hodson, E. L., Houweling, S., Josse, B., Fraser, P. J., Krummel, P. B., Lamarque, J. F., Langenfelds, R. L., Le Quere, C., Naik, V., O’Doherty, S., Palmer, P. I., Pison, I., Plummer, D., Poulter, B., Prinn, R. G., Rigby, M., Ringeval, B., Santini, M., Schmidt, M., Shindell, D. T., Simpson, I. J., Spahni, R., Steele, L. P., Strode, S. A., Sudo, K., Szopa, S., van der Werf, G. R., Voulgarakis, A., van Weele, M., Weiss, R. F., Williams, J. E., and Zeng, G.: Three decades of global methane sources and sinks, *Nat. Geosci.*, 6, 813–823, <https://doi.org/10.1038/ngeo1955>, 2013.

- Lahteenoja, O. and Page, S.: High diversity of tropical peatland ecosystem types in the Pastaza-Maranon basin, Peruvian Amazonia, *J. Geophys. Res.-Biogeo.*, 116, 1–14, <https://doi.org/10.1029/2010jg001508>, 2011.
- Lähteenoja, O. and Roucoux, K.: Inception, history and development of peatlands in the Amazon Basin, *PAGES News*, 18, 27–31, 2010.
- Lahteenoja, O., Ruokolainen, K., Schulman, L., and Alvarez, J.: Amazonian floodplains harbour minerotrophic and ombrotrophic peatlands, *Catena*, 79, 140–145, <https://doi.org/10.1016/j.catena.2009.06.006>, 2009a.
- Lahteenoja, O., Ruokolainen, K., Schulman, L., and Oinonen, M.: Amazonian peatlands: an ignored C sink and potential source, *Global Change Biol.*, 15, 2311–2320, <https://doi.org/10.1111/j.1365-2486.2009.01920.x>, 2009b.
- Lahteenoja, O., Reategui, Y. R., Rasanen, M., Torres, D. D., Oinonen, M., and Page, S.: The large Amazonian peatland carbon sink in the subsiding Pastaza-Maranon foreland basin, Peru, *Global Change Biol.*, 18, 164–178, <https://doi.org/10.1111/j.1365-2486.2011.02504.x>, 2012.
- Lavelle, P., Rodriguez, N., Arguello, O., Bernal, J., Botero, C., Charparro, P., Gomez, Y., Gutierrez, A., Hurtado, M. D., Loaiza, S., Pullido, S. X., Rodriguez, E., Sanabria, C., Velasquez, E., and Fonte, S. J.: Soil ecosystem services and land use in the rapidly changing Orinoco River Basin of Colombia, *Agr. Ecosyst. Environ.*, 185, 106–117, <https://doi.org/10.1016/j.agee.2013.12.020>, 2014.
- Liengaard, L., Nielsen, L. P., Revsbech, N. P., Priem, A., Elberling, B., Enrich-Prast, A., and Kuhl, M.: Extreme emission of N<sub>2</sub>O from tropical wetland soil (Pantanal, South America), *Front. Microbiol.*, 3, 1–13, <https://doi.org/10.3389/fmicb.2012.00433>, 2013.
- Limpens, J., Berendse, F., Blodau, C., Canadell, J. G., Freeman, C., Holden, J., Roulet, N., Rydin, H., and Schaepman-Strub, G.: Peatlands and the carbon cycle: from local processes to global implications – a synthesis, *Biogeosciences*, 5, 1475–1491, <https://doi.org/10.5194/bg-5-1475-2008>, 2008.
- Livingston, G. and Hutchinson, G.: Chapter 2: Enclosure-based measurement of trace gas exchange: applications and sources of error, in: *Biogenic Trace Gases: Measuring Emissions from Soil and Water*, edited by: Matson, P. and Harriss, R. C., Blackwell Science Ltd, Cambridge, MA, USA, 14–51, 1995.
- Marani, L. and Alvalá, P. C.: Methane emissions from lakes and floodplains in Pantanal, Brazil, *Atmos. Environ.*, 41, 1627–1633, <https://doi.org/10.1016/j.atmosenv.2006.10.046>, 2007.
- McClain, M. E., Boyer, E. W., Dent, C. L., Gergel, S. E., Grimm, N. B., Groffman, P. M., Hart, S. C., Harvey, J. W., Johnston, C. A., Mayorga, E., McDowell, W. H., and Pinay, G.: Biogeochemical hot spots and hot moments at the interface of terrestrial and aquatic ecosystems, *Ecosystems*, 6, 301–312, <https://doi.org/10.1007/s10021-003-0161-9>, 2003.
- Melack, J. M., Hess, L. L., Gastil, M., Forsberg, B. R., Hamilton, S. K., Lima, I. B. T., and Novo, E.: Regionalization of methane emissions in the Amazon Basin with microwave remote sensing, *Global Change Biol.*, 10, 530–544, <https://doi.org/10.1111/j.1529-8817.2003.00763.x>, 2004.
- Melton, J. R., Wania, R., Hodson, E. L., Poulter, B., Ringeval, B., Spahni, R., Bohn, T., Avis, C. A., Beerling, D. J., Chen, G., Eliseev, A. V., Denisov, S. N., Hopcroft, P. O., Lettenmaier, D. P., Riley, W. J., Singarayer, J. S., Subin, Z. M., Tian, H., Zurcher, S., Brovkin, V., van Bodegom, P. M., Kleinen, T., Yu, Z. C., and Kaplan, J. O.: Present state of global wetland extent and wetland methane modelling: conclusions from a model inter-comparison project (WETCHIMP), *Biogeosciences*, 10, 753–788, <https://doi.org/10.5194/bg-10-753-2013>, 2013.
- Morley, N. and Baggs, E. M.: Carbon and oxygen controls on N<sub>2</sub>O and N<sub>2</sub> production during nitrate reduction, *Soil Biol. Biochem.*, 42, 1864–1871, <https://doi.org/10.1016/j.soilbio.2010.07.008>, 2010.
- Morton, D. C., Nagol, J., Carabajal, C. C., Rosette, J., Palace, M., Cook, B. D., Vermote, E. F., Harding, D. J., and North, P. R. J.: Amazon forests maintain consistent canopy structure and greenness during the dry season, *Nature*, 506, 221–224, <https://doi.org/10.1038/nature13006>, 2014.
- Murphy, W. A., Berrio, J. C., Boom, A., Page, S. E., and Teh, Y. A.: Spatial and diurnal trends in methane and nitrous oxide flux within peatland ecosystems, in: *Methane emissions from peat swamp forests of differing vegetation types, within the Loreto Region of the Peruvian Amazonas – unpublished PhD thesis*, University of Leicester, Leicester, 2017.
- Nisbet, E. G., Dlugokencky, E. J., and Bousquet, P.: Methane on the Rise – Again, *Science*, 343, 493–495, <https://doi.org/10.1126/science.1247828>, 2014.
- Pangala, S. R., Moore, S., Hornibrook, E. R. C., and Gauci, V.: Trees are major conduits for methane egress from tropical forested wetlands, *New Phytol.*, 197, 524–531, <https://doi.org/10.1111/nph.12031>, 2013.
- Pett-Ridge, J., Petersen, D. G., Nuccio, E., and Firestone, M. K.: Influence of oxic/anoxic fluctuations on ammonia oxidizers and nitrification potential in a wet tropical soil, *FEMS Microbiol. Ecol.*, 85, 179–194, <https://doi.org/10.1111/1574-6941.12111>, 2013.
- Prosser, J. I. and Nicol, G. W.: Relative contributions of archaea and bacteria to aerobic ammonia oxidation in the environment, *Environ. Microbiol.*, 10, 2931–2941, <https://doi.org/10.1111/j.1462-2920.2008.01775.x>, 2008.
- Pumpanen, J., Kolari, P., Ilvesniemi, H., Minkkinen, K., Vesala, T., Niinistö, S., Lohila, A., Larmola, T., Morero, M., Pihlatie, M., Janssens, I., Yuste, J. C., Grünzweig, J. M., Reth, S., Subke, J.-A., Savage, K., Kutsch, W., Øzstreg, G., Ziegler, W., Anthoni, P., Lindroth, A., and Hari, P.: Comparison of different chamber techniques for measuring soil CO<sub>2</sub> efflux, *Agr. Forest Meteorol.*, 123, 159–176, <https://doi.org/10.1016/j.agrformet.2003.12.001>, 2004.
- Saikawa, E., Schlosser, C. A., and Prinn, R. G.: Global modeling of soil nitrous oxide emissions from natural processes, *Global Biogeochem. Cy.*, 27, 972–989, <https://doi.org/10.1002/gbc.20087>, 2013.
- Saikawa, E., Prinn, R. G., Dlugokencky, E., Ishijima, K., Dutton, G. S., Hall, B. D., Langenfelds, R., Tohjima, Y., Machida, T., Manizza, M., Rigby, M., O’Doherty, S., Patra, P. K., Harth, C. M., Weiss, R. F., Krummel, P. B., van der Schoot, M., Fraser, P. J., Steele, L. P., Aoki, S., Nakazawa, T., and Elkins, J. W.: Global and regional emissions estimates for N<sub>2</sub>O, *Atmos. Chem. Phys.*, 14, 4617–4641, <https://doi.org/10.5194/acp-14-4617-2014>, 2014.
- Saleska, S. R., Wu, J., Guan, K., Araujo, A. C., Huete, A., Nobre, A. D., and Restrepo-Coupe, N.: Dry-season

- greening of Amazon forests, *Nature*, 531, E4–E5, <https://doi.org/10.1038/nature16457>, 2016.
- Sawakuchi, H. O., Bastviken, D., Sawakuchi, A. O., Krusche, A. V., Ballester, M. V. R., and Richey, J. E.: Methane emissions from Amazonian Rivers and their contribution to the global methane budget, *Global Change Biol.*, 20, 2829–2840, <https://doi.org/10.1111/gcb.12646>, 2014.
- Schlesinger, W. H.: An estimate of the global sink for nitrous oxide in soils, *Global Change Biol.*, 19, 2929–2931, <https://doi.org/10.1111/gcb.12239>, 2013.
- Schulman, L., Ruokolainen, K., and Tuomisto, H.: Parameters for global ecosystem models, *Nature*, 399, 535–536, 1999.
- Silver, W. L., Lugo, A., and Keller, M.: Soil oxygen availability and biogeochemistry along rainfall and topographic gradients in upland wet tropical forest soils, *Biogeochemistry*, 44, 301–328, 1999.
- Silver, W. L., Herman, D. J., and Firestone, M. K. S.: Dissimilatory Nitrate Reduction to Ammonium in Upland Tropical Forest Soils, *Ecology*, 82, 2410–2416, 2001.
- Sjögersten, S., Black, C. R., Evers, S., Hoyos-Santillan, J., Wright, E. L., and Turner, B. L.: Tropical wetlands: A missing link in the global carbon cycle?, *Global Biogeochem. Cy.*, 28, 1371–1386, <https://doi.org/10.1002/2014GB004844>, 2014.
- Smith, L. K., Lewis, W. M., Chanton, J. P., Cronin, G., and Hamilton, S. K.: Methane emissions from the Orinoco River floodplain, Venezuela, *Biogeochemistry*, 51, 113–140, 2000.
- Strack, M., Kellner, E., and Waddington, J. M.: Dynamics of biogenic gas bubbles in peat and their effects on peatland biogeochemistry, *Global Biogeochem. Cy.*, 19, 1–9, <https://doi.org/10.1029/2004GB002330>, 2005.
- Teh, Y. A. and Silver, W. L.: Effects of soil structure destruction on methane production and carbon partitioning between methanogenic pathways in tropical rain forest soils, *J. Geophys. Res.-Biogeo.*, 111, 1–8, <https://doi.org/10.1029/2005JG000020>, 2006.
- Teh, Y. A., Silver, W. L., and Conrad, M. E.: Oxygen effects on methane production and oxidation in humid tropical forest soils, *Global Change Biol.*, 11, 1283–1297, <https://doi.org/10.1111/j.1365-2486.2005.00983.x>, 2005.
- Teh, Y. A., Silver, W. L., Conrad, M. E., Borglin, S. E., and Carlson, C. M.: Carbon isotope fractionation by methane-oxidizing bacteria in tropical rain forest soils, *J. Geophys. Res.-Biogeo.*, 111, 1–8, <https://doi.org/10.1029/2005jg000053>, 2006.
- Teh, Y. A., Dubinsky, E. A., Silver, W. L., and Carlson, C. M.: Suppression of methanogenesis by dissimilatory Fe(III)-reducing bacteria in tropical rain forest soils: implications for ecosystem methane flux, *Global Change Biol.*, 14, 413–422, <https://doi.org/10.1111/j.1365-2486.2007.01487.x>, 2008.
- Teh, Y. A., Silver, W. L., Sonnentag, O., Detto, M., Kelly, M., and Baldocchi, D. D.: Large Greenhouse Gas Emissions from a Temperate Peatland Pasture, *Ecosystems*, 14, 311–325, <https://doi.org/10.1007/s10021-011-9411-4>, 2011.
- Teh, Y. A., Diem, T., Jones, S., Huaraca Quispe, L. P., Baggs, E., Morley, N., Richards, M., Smith, P., and Meir, P.: Methane and nitrous oxide fluxes across an elevation gradient in the tropical Peruvian Andes, *Biogeosciences*, 11, 2325–2339, <https://doi.org/10.5194/bg-11-2325-2014>, 2014.
- Tian, H., Melillo, J. M., Kicklighter, D. W., McGuire, A. D., Helfrich III, J. V. K., Moore III, B., and Vorosmarty, C. J.: Effect of interannual climate variability on carbon storage in Amazonian ecosystems, *Nature*, 396, 664–667, 1998.
- von Fischer, J. and Hedin, L.: Separating methane production and consumption with a field-based isotope dilution technique, *Global Biogeochem. Cy.*, 16, 1–13, <https://doi.org/10.1029/2001GB001448>, 2002.
- von Fischer, J. C. and Hedin, L. O.: Controls on soil methane fluxes: Tests of biophysical mechanisms using stable isotope tracers, *Global Biogeochem. Cy.*, 21, 9, Gb2007, <https://doi.org/10.1029/2006gb002687>, 2007.
- Wen, Y., Chen, Z., Dannenmann, M., Carminati, A., Willibald, G., Kiese, R., Wolf, B., Veldkamp, E., Butterbach-Bahl, K., and Corre, M. D.: Disentangling gross N<sub>2</sub>O production and consumption in soil, *Sci. Rep.*, 6, 8, <https://doi.org/10.1038/srep36517>, 2016.
- Werner, C., Butterbach-Bahl, K., Haas, E., Hickler, T., and Kiese, R.: A global inventory of N<sub>2</sub>O emissions from tropical rainforest soils using a detailed biogeochemical model, *Global Biogeochem. Cy.*, 21, Gb3010, <https://doi.org/10.1029/2006gb002909>, 2007.
- Whalen, S. C.: Biogeochemistry of methane exchange between natural wetlands and the atmosphere, *Environ. Eng. Sci.*, 22, 73–94, <https://doi.org/10.1089/ees.2005.22.73>, 2005.
- Whiting, G. J. and Chanton, J. P.: Primary production control of methane emission from wetlands, *Nature*, 364, 794–795, 1993.
- Wilson, C., Gloor, M., Gatti, L. V., Miller, J. B., Monks, S. A., McNorton, J., Bloom, A. A., Basso, L. S., and Chipperfield, M. P.: Contribution of regional sources to atmospheric methane over the Amazon Basin in 2010 and 2011, *Global Biogeochem. Cy.*, 30, 400–420, <https://doi.org/10.1002/2015GB005300>, 2016.
- Wright, E. L., Black, C. R., Cheesman, A. W., Drage, T., Large, D., Turner, B. L., and Sjögersten, S.: Contribution of subsurface peat to CO<sub>2</sub> and CH<sub>4</sub> fluxes in a neotropical peatland, *Global Change Biol.*, 17, 2867–2881, <https://doi.org/10.1111/j.1365-2486.2011.02448.x>, 2011.
- Yang, W. H., Teh, Y. A., and Silver, W. L.: A test of a field-based N<sub>15</sub>-nitrous oxide pool dilution technique to measure gross N<sub>2</sub>O production in soil, *Global Change Biol.*, 17, 3577–3588, <https://doi.org/10.1111/j.1365-2486.2011.02481.x>, 2011.
- Ye, R. and Horwath, W. R.: Nitrous oxide uptake in rewetted wetlands with contrasting soil organic carbon contents, *Soil Biol. Biochem.*, 100, 110–117, <https://doi.org/10.1016/j.soilbio.2016.06.009>, 2016.